New Approaches to Chemical Patterns

Barry R. Johnson and Stephen K. Scott
School of Chemistry, University of Leeds, Leeds, UK, LS2 9JT

1 Introduction

For many people, the patterns of 'chemical gardens', rock strata and their laboratory equivalents Liesgang Rings are as an important a part of the early attraction of chemistry as 'smells and bangs.' These 'reaction–diffusion structures' arise from a cooperation between molecular transport through diffusion and chemical kinetics. In recent years there has been considerable interest [1–3] in the study of chemical patterns fuelled by an almost casual suggestion[4] of one of Britain's more enigmatic mathematicians and made possible by rapid advances in technology driven by several groups of imaginative chemists. In this review, we survey the various new observations made along the route to taming of so-called 'Turing Structures' in the laboratory and attempt to set these in the context of their relevance in chemistry and other areas of science.

2 Background concepts

2.1 Chemical Feedback

In all but the simplest (elementary) reaction systems many different species become involved during the course of the conversion of the initial reactants to the final products. Species which are formed in early stages but then react further are termed *intermediates* and are frequently more reactive than their precursors. In such systems, we can still define a *reaction rate* in terms of the rate at which the concentration of one of the initial reactants is decreasing in time or as the rate at which the concentration of one of the final products is increasing. The way in which this rate varies during the reaction can be examined by plotting it against the *extent* or fractional conversion of the initial reactant. In some cases, these rate–extent curves have one of the shapes shown in Fig. 1(*a*). These correspond to so-called *deceleratory* kinetics, as the reaction rate falls steadily throughout the whole course of the reaction, having its maximum value at the very start. Such rate–extent curves are often represented by simple n-th order rate laws, with $n = 1$ for a first-order reaction, $n = 2$ for second-order and so on.

The rate–extent curves in Fig. 1(*b*) have a different form in that they show the reaction rate *increasing* with the extent, at least in the early stages, and so have an *acceleratory* phase, before attaining a maximum when perhaps half of the reactants have been consumed.

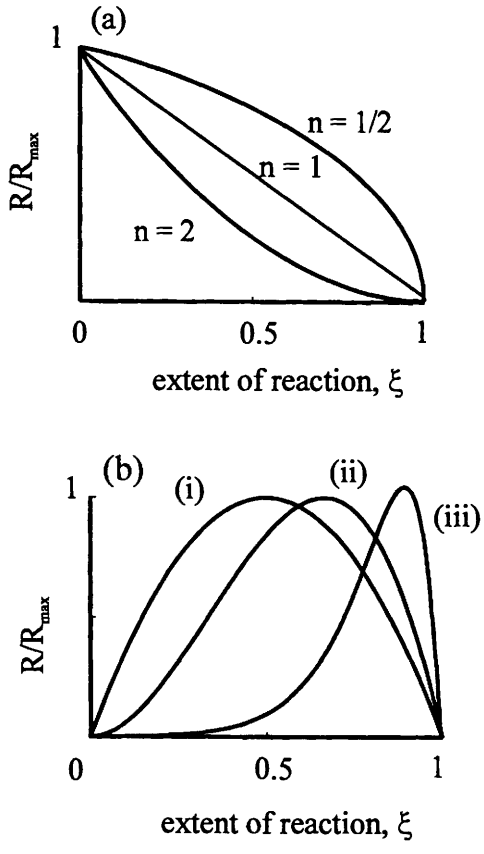

Figure 1 (a) Dependence of reaction rate on extent of conversion, ξ, for different order of deceleratory reactions. The rate is normalised to the maximum rate, R_{max}, which for these systems corresponds to $\xi = 0$. (b) Reaction rate dependence on the extent of conversion for (i) quadratic and (ii) cubic autocatalysis, and (iii) an exothermic reaction illustrating the different positions of maximum reaction rate for feedback systems.

Barry R. Johnson

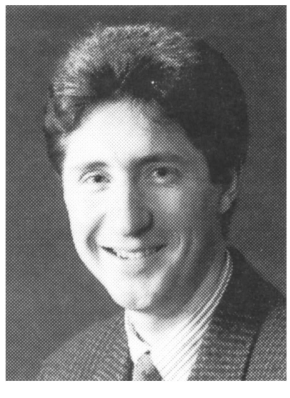

Stephen K. Scott

Stephen Scott is Professor of Mathematical Chemistry and currently Head of Physical Chemistry at the University of Leeds where he and Dr Barry Johnson run the 'Nonlinear Kinetics Laboratory'. Both authors are Leeds graduates: Scott has had periods in Australia (postdoc) and USA (Fulbright Professor); Johnson was a postdoc at Stanford. Our research areas include oscillating reactions, chemical waves and the applications of chaos theory in which areas we have written several books in recent years.

Such curves indicate the existence of some *chemical feedback* process in the reaction mechanism. A simplified but very useful representation of chemical feedback based on *autocatalysis*[3] imagines a reaction in which some chemical A is converted to a product B but for which the reaction rate increases as the product concentration increases as if B plays the role of a catalyst for its own production. Two basic forms are often exploited:

quadratic autocatalysis	$A + B \rightarrow 2B$	$\text{rate} = k_q ab$	(1)
cubic autocatalysis	$A + 2B \rightarrow 3B$	$\text{rate} = k_c ab^2$	(2)

where a and b are the concentrations of the reactant and autocatalyst and k_q and k_c are rate constants.

Whilst there is almost certainly no actual chemical reaction in which such a conversion occurs in a single elementary step, the rate–extent curves for a considerable (and ever-growing) class of reactions can be fitted by one or other of these caricatures (or by a combination of the two). The autocatalyst B is frequently referred to as the *feedback* species or *activator*. In some cases it is relevant to identify an *inhibitor* species from amongst the reactants, whose removal has an overall accelerating effect on the reaction.

2.2 Examples of Systems showing Chemical Feedback

Chemical feedback forms the kinetic clockwork driving various 'exotic' types of reaction behaviour, including oscillations. At the time of Alan Turing's paper (1952) there was no well-established example of an oscillatory reaction although Boris Belousov had made an initial attempt the previous year to publish his observations concerning the reaction that now bears his name in conjunction with Anatol Zhabotinsky. The 'BZ' reaction is now a familiar lecture demonstration with its repetitive red–blue–red oscillations that last for several hours in a well-stirred beaker and many other chemical reactions with feedback are now very well-characterised: feedback is far from a rarity in chemical kinetics.

The BZ reaction[3] involves the oxidation of a suitable organic substrate, often malonic (propane-1,3-dioic) acid with an acidified bromate solution in the presence of a transition metal redox catalyst such as the ferroin-ferriin couple, in which Fe is complexed with 1,10-phenanthroline and oscillates between the red Fe^{II} and blue Fe^{III} states. The important features of the mechanism of the BZ system are now relatively firmly established: there are essentially three important overall processes: an inhibition phase involving bromide ion, an autocatalytic phase in which the redox catalyst is oxidised, and a clock-resetting phase in which bromide ion is produced as the redox catalyst is reduced. The autocatalytic species has been identified as $HBrO_2$, and the autocatalytic phase has the overall stoichiometry:

$$BrO_3^- + HBrO_2 + 3H^+ + 2Fe^{II} \rightarrow 2HBrO_2 + 2Fe^{III} + H_2O$$
$$\text{rate} = k\,[BrO_3^-][HBrO_2][H^+]^2$$

thus exhibiting the quadratic-type of kinetics in eqn. (1), with the reactant A corresponding to bromate ion.

If a solution of BZ reagents is spread as a thin layer in a Petri dish, waves of the oxidation reaction spread out from certain *pacemaker* sites,[5] which perhaps correspond to sites where the local pH varies from that of the bulk (these may arise from dust particles or defects in the dish surface). The waves appear as thin blue reaction zones moving across a red background often as concentric circles (*target patterns*) or as *spiral waves*, examples of which are shown in Fig. 2. Spirals and targets occur more widely in chemistry and biology: recent work has shown that the reaction of CO with O atoms on some Pt crystal planes occurs through spiral waves on the crystal surface;[6] spirals and targets have very recently been reported in gas-phase reaction;[7] the slime mould *Dictyostelium discoideum* responds to starvation by changing from a colony of individual single cells into a multicellular organism,[8] with the cells coming together under the influence of chemical signalling and *chemotaxis* in a spiralling migration; spirals and their three-dimensional counterparts, scroll waves, are implicated in disorders of the heart and may be associated with epileptic seizures.[9]

Despite their names, these are not chemical 'patterns' in the Turing sense; the exact spatial distribution depends crucially on the chance locations of the pacemaker sites rather than just the underlying kinetics and the reaction zone size. They are, nevertheless, attractive and important examples of chemical spatiotemporal organisation.

A second solution-phase reaction that has become increasingly exploited for studies of spatial patterning is the CIMA (chlorite–iodide–malonic acid) reaction[10] or its close cousin the CDIMA (chlorine dioxide–iodine–malonic acid) system. These differ only in the precise chemical form in which the oxychlorine and iodine reagents are supplied: in the CIMA system, the initial ClO_2^- and I^- are almost completely consumed during a pre-oscillatory induction phase during which ClO_2 and I_2 are the major 'reactant' species with chlorite and iodide acting as the 'intermediates'. The Lengyel–Rabai–Epstein[11] mechanism for this reaction involves three component processes:

(CIMA1) $MA + I_2 \rightarrow IMA + I^- + H^+$
$\text{rate} = k_{1a}[MA][I_2]/(k_{1b} + [I_2])$

(CIMA2) $ClO_2 + I^- \rightarrow ClO_2^- + \tfrac{1}{2}I_2$
$\text{rate} = k_2[ClO_2][I^-]$

(CIMA3) $ClO_2^- + 4I^- + 4H^+ \rightarrow 2I_2 + Cl^- + 2H_2O$
$\text{rate} = k_{3a}[ClO_2^-][I^-]H^+ + k_{3b}[ClO_2^-][I_2][I^-]/(\alpha + [I^-]^2)$

The empirical rate laws for each of these overall stoichiometries indicate that there is a complex role for I_2 in (CIMA1) and that I_2 acts as an autocatalyst in (CIMA3) in which iodide ion is an inhibitor. Under the normal reaction conditions, I_2 is present in excess and its concentration is effectively constant, so the inhibitory role of I^- is the dominant feedback route.

The CIMA reaction also exhibits oscillations in well-stirred batch reactors and target 'patterns' in unstirred systems: using starch as an indicator the reaction varies between blue (reduced state) and clear/pale yellow (oxidised state).

2.3 Diffusion-driven Instabilities: Turing Patterns

In most simple situations, diffusion has a 'smoothing out' effect which serves to produce uniform spatial distributions of chemical species as time progresses: a simple example is the spread of a drop of ink in a beaker of water to produce a dilute, uniform ink solution. The possibility of the reverse process, all the ink particles spontaneously gathering together in some small region of the solution and leaving the bulk colourless, is usually viewed as that most heinous of suggestions – a violation of The Second Law of Thermodynamics. Alan Turing's startling prediction[4] was that if diffusion is coupled with chemical feedback, then something similar to this spatial organisation can indeed occur spontaneously, without invoking demons or violating the Second Law. Subsequent theoretical work by Prigogine's group in Brussels and by others elsewhere showed that chemical reactions would be an ideal hunting ground for Turing Patterns.

The basic requirements for a system to decide to self-organise from an initially uniform distribution of all concentrations into a situation where some species have concentrations that vary with position are that: (*i*) the feedback process be sufficiently strong that it can support oscillations under well-stirred conditions and (*ii*) the diffusion coefficient for the feedback species should be less than that for the inhibitor–reactant species, *i.e.* we require $D_B/D_A < 1$. It might be imagined that some reactions might meet this naturally (*e.g.* if they involve molecules of distinctly different molar masses), but in general the need *selectively* to control one diffusion coefficient in a reacting system has presented a problem that has only recently been resolved.

There are some subsidiary requirements: diffusion is a relatively weak process and the frail chemical patterns that arise from its coupling with feedback kinetics are readily disrupted by fluid motion whether imposed or arising as a consequence of the chemistry. The latter situation can arise relatively easily in reactions as a result of density changes accompanying the reaction that, in turn, may be caused by a reaction that is exothermic and thus having local self-

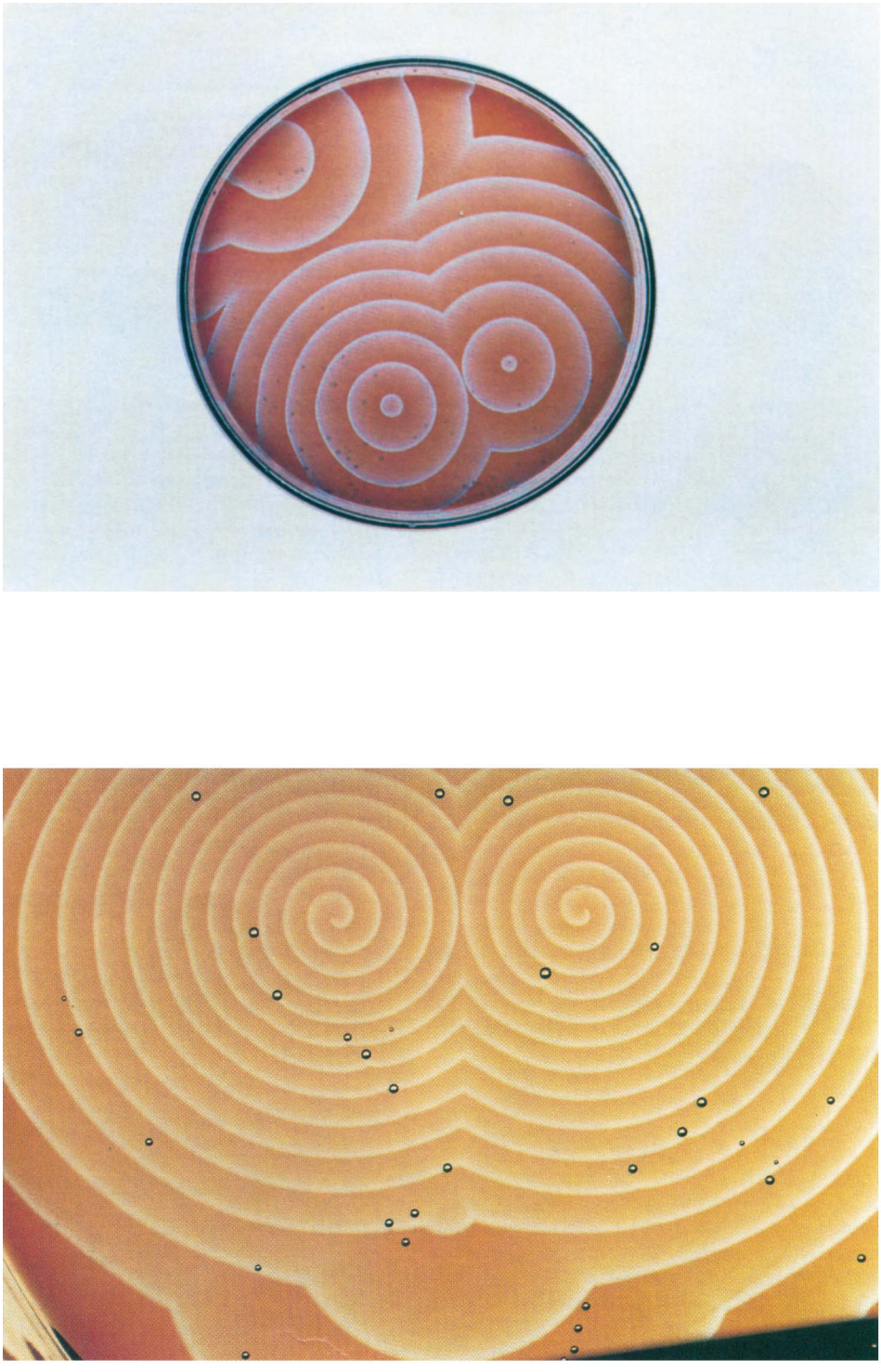

Figure 2 (Top) Target patterns formed in a thin layer of BZ reaction mixture, 7.25 min after mixing. There are three random pacemaker sites in the 9 cm diameter Petri dish. (Bottom) Spiral waves formed by breaking target patterns. Each spiral rotates with the same period (30 s) and has the same frequency.

heating where the reaction rate is highest or if there is a change in the molar volume in going from reactants to products. In either case, the density changes will lead to convective motion of the solution; this itself can give rise to some interesting spatial phenomena, and chemical reactions which have suitable colour changes can be used to reveal such induced convection, but it is separate from the diffusion-driven Turing mechanism.

A second requirement is for a continuous supply of fresh reactants (and a matching removal of products if the volume of the system is not to grow). This flow allows the system to sustain a pattern indefinitely, driven by the free energy change accompanying the reaction; in the absence of flow, patterns may develop during the reaction but they are inevitable transient phenomena and the system returns to spatial uniformity as the system approaches its chemical equilibrium state. These two different requirements – the provision of a continuous supply but also the suppression of fluid motion – are, to some extent, contradictory and represented a considerable challenge to the experimental verification of Turing's predictions.

Systems that meet the various conditions set out above should show spontaneous spatial organisation to produce chemical patterns that have a 'natural wavelength' that depend on the reaction kinetic parameters (rate constants *etc.*) and on the diffusion coefficients. The wavelength is mainly independent of the size of the reaction

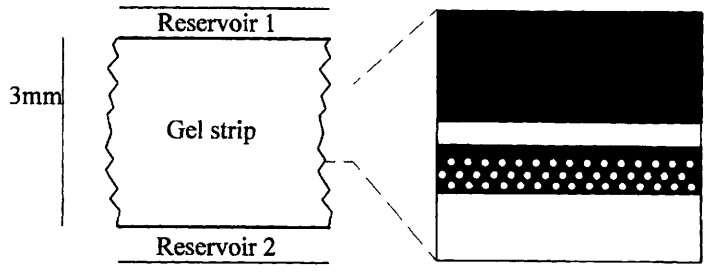

Figure 3 The Gel Strip reactor and the first experimental Turing Pattern in the CIMA reaction (left) Sketch of the reactor Reagents are well mixed in the reservoirs, 1 and 2 and diffuse into the gel from the longest edges (right) Contrast enhanced picture of Turing pattern several rows of clear spots where dark regions correspond to reduced state, clear regions correspond to oxidised state Experimental conditions temperature 7 °C, boundary feed conditions (concentrations in mol l^{-1}) $[NaClO_2] = 2.6 \times 10^{-2}$, $[KI] = 3 \times 10^{-3}$, $[NaOH] = 3 \times 10^{-3}$, $[Na_2SO_4] = 3 \times 10^{-3}$, $[CH_2(COOH)_2 = 9 \times 10^{-3}$, $[H_2SO_4] = 1 \times 10^{-2}$ (Reproduced with permission from Castets *et al* [13] © The American Physical Society)

zone, although there is a need for this to exceed some minimum dimension in order that at least one half-wavelength can be accommodated If this condition is met, then patterns may be expected provided the concentrations of the major reactant species lie in certain ranges, *i e* patterns are only found over finite ranges of experimental conditions

Any patterning that does develop needs to be recorded in some way The technology for such image capturing and processing has been brought to a very sophisticated state based on video camera + frame digitisation techniques pioneered in the chemical context by the group of Benos Hess, Stefan Muller and Theo Plesser at Dortmund [12] These provide essentially spatially and temporally resolved spectrophotometry with intensity levels as a function of position and time that can be converted to absolute concentrations if required or simply used as grey-scale monitors of changes in signal

3 The First Experimental Observations of Turing Patterns

Various new experimental configurations have been designed and tested in order to satisy the demands listed in the previous section Central to the success in the search for Turing Patterns has been the use of gels instead of an aqueous solution phase These were primarily adopted to reduce the tendency for natural convective motion and also to allow streams of fresh reactants to flow past the reaction zone without disrupting the diffusive transport within the matrix

3.1 The Gel Strip Reactor

The Gel Strip Reactor[13] devised by the group of Jacques Boissonade and Patrick De Kepper in Bordeaux consists of a narrow, rectangular piece of polyacrylamide hydrogel approximately 20 mm in length and 3 mm wide (with a thickness of 1 mm) The two long edges are placed in contact with separate reservoirs of reactant species, as indicated in Fig 3, in which the concentrations are maintained constant by continuous flow Diffusion of the individual reactant species occurs across the strip, so there are natural concentration gradients in this system perpendicular to the reservoirs, but not in a direction parallel to the long edges Reaction occurs in the gel strip where the concentrations of all species are non-zero

In order to render the development of the reaction visible by eye and to a standard video camera imaging system, the gel can be loaded with suitable indicators such as starch or thiodene This apparently simple device has an initially unsuspected advantage The feedback species for the CIMA reaction is I^- which in the presence of I_2 forms I_3^- This species complexes with the starch or other indicator which itself is a large molecule and which has a low mobility in the gel matrix The I_3 indicator complex thus has a reduced effective diffusion coefficient[14] whilst other species have diffusion coefficients that are substantially higher (the diffusivities of 'normal size' molecules in the gel are approximately equal to their solution-phase values) In this way, the system is arranged to satisfy the Turing requirement in terms of differing diffusivities

The first experimental examples of a Turing Pattern obtained in this way[13] are shown in Fig 3 The spatial structure perpendicular to the long edges is, as explained above, driven at least in part by the imposed chemical gradients, but the spatial inhomogeneity along the strip, right-to-left in the figure must arise from a Turing mechanism based on feedback reaction and selective diffusion The wavelength scale of the pattern is of the order of 0 2 mm and hence much smaller than the reactor dimensions, suggesting that the strip geometry has no determining role in the pattern

By varying the concentrations of individual reactants in the reservoirs, different spatial structures can be obtained,[15] as indicated in Fig 4 In this figure, the main change with composition lies in the number of 'fronts', *i e* changes from oxidised to the reduced state, lying parallel to the reservoirs (so the spatial structure is parallel to the imposed concentration gradients), with the Turing Pattern-type spots only occurring in region IV The investigation of other types of Turing Pattern has been pursued with a different type of gel reactor

3.2 The Gel Disk Reactor

A variation on the Gel Strip Reactor developed by Qi Ouyang and Harry Swinney in Texas involves a disk of the gel matrix separating different reactant reservoirs of constant concentration[16,17] (maintained by continuous flow), with the reaction then monitored by video camera as indicated in Fig 5(*a*)

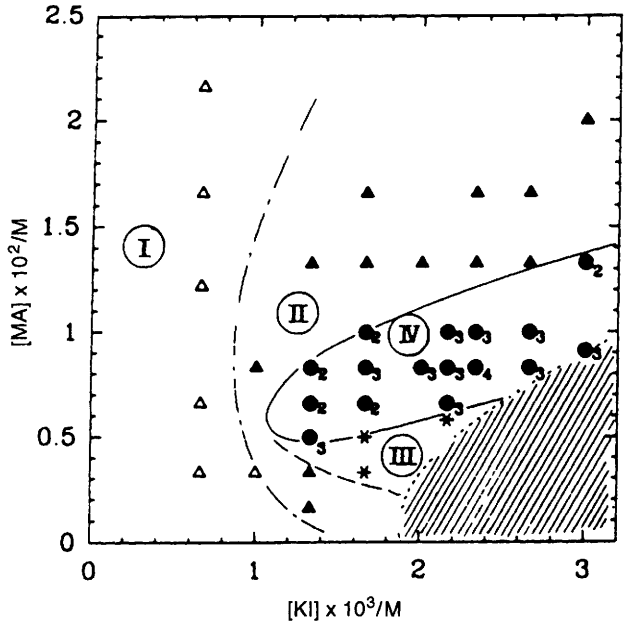

Figure 4 Phase diagram of sustained patterns Section in the plane (iodide–malonic acid) Regions I single front pattern, II triple front pattern, III multiple front pattern, IV spot pattern Numbers next to symbols indicate the number of rows Experimental conditions temperature 4°C, other parameters as for Fig 3 (Reproduced with permission from Castets *et al* [15] © 1990 The American Physical Society)

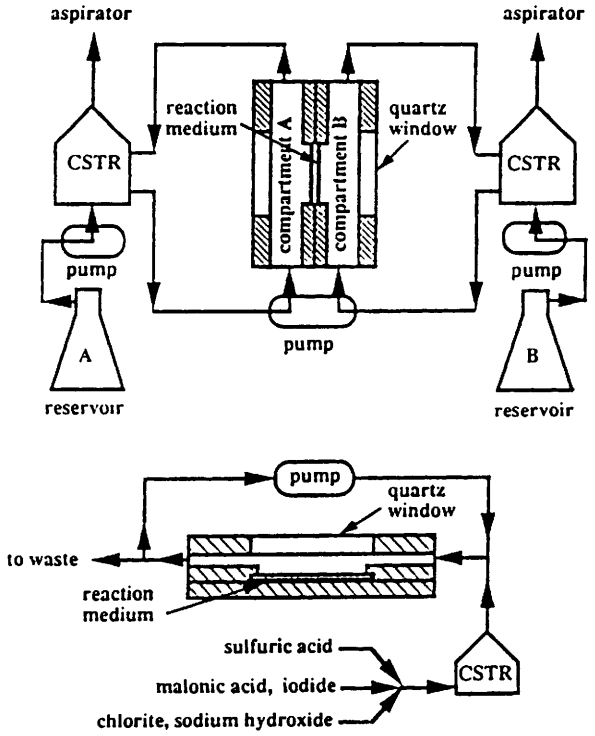

Figure 5 Schematic diagrams of open spatial reactors fed by cstrs. (a) Two-side fed reactor and (b) one-side fed reactor. (Reproduced with permission from Ouyang *et al.*[16,17] (a) © 1991 American Institute of Physics, (b) © 1992 Elsevier Science BV)

A further variation on this is the single-side feed, Fig. 5(*b*), in which the reactants are mixed prior to entering the chamber above the gel in which the mixture has a relatively short residence time. Again, an indicator can be incorporated into the gel although polyvinyl alcohol gels are self-indicating and also play the role of reducing the mobility of the feedback species. The system is viewed along the imposed concentration gradients and so any patterns that are observed lie perpendicular to these gradients and arise from the Turing mechanism.

As shown in Fig. 6, changing the reservoir concentration can cause the pattern to change from a hexagonal arrangement of 'spots' to 'stripes' much as predicted in the Turing theory. Rhombic arrangements of spots and 'zig-zag' arrangements of stripes have also been observed as the reactant concentrations are varied.[18]

Subsequent studies by Agaldze *et al.*[19] in which the reaction occurs in capillary tubes have indicated that the precise form of the gel is not vital for Turing patterns, and even that the patterns can arise without a gel, indicating that the starch–iodine complex is sufficiently less mobile than IO_3^- in aqueous solution for the requirement of different diffusivities to be met.

4 Patterning in Reaction Fronts and Flames

The kinetics required to support oscillatory behaviour in batch systems represent one degree of complexity up from the simple one-off feedback processes represented in eqns. (1) and (2). A single autocatalytic process can, however, support a one-off clock reaction in which there is a rapid reaction event at the end of a long induction period. If such a system is conducted in an unstirred solution and the reaction is initiated locally in a small region, then a one-off reaction-diffusion *front* can emerge in which the diffusion of the autocatalyst triggers reaction in the surrounding region. Such fronts are isothermal analogues of flames in which the primary feedback arises thermally from the exothermicity of the reaction.

In the simplest circumstances, fronts propagate as circles or spheres (in 2D and 3D reaction zones) or as a planar front. However, if the diffusivities of the reactant and feedback species can be made to differ, there can be a spontaneous development of more complex wave front geometries. This effect was first observed and analysed in flame systems, but has also recently been demonstrated[20] experimentally for a chemical feedback system. The reaction between iodate and iodide ion in acidified solution in the presence of the suit-

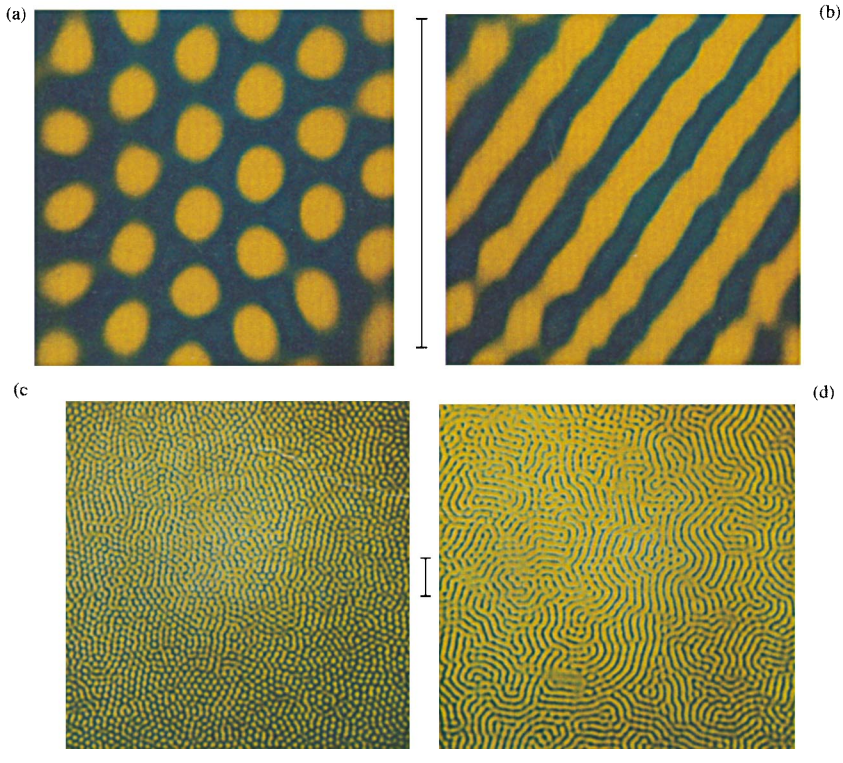

Figure 6 Stationary chemical patterns formed in the two-side fed open reactor with a polyacrylamide gel: (a) and (c) hexagons; (b) and (d) stripes. The bar beside each picture represents 1 mm. The concentrations (in mol l^{-1}) in reservoirs A and B were (a) $[I^-] = 3.0 \times 10^{-3}$, $[CH_2(COOH)_2] = 1.3 \times 10^{-2}$ and (b) $[I^-] = 5.0 \times 10^{-3}$, $[CH_2(COOH)_2] = 8.3 \times 10^{-2}$ with the other parameters held fixed at $[Na_2SO_4] = 4.5 \times 10^{-3}$, $[ClO_2^-] = 1.8 \times 10^{-2}$, $[H_2SO_4]_A = 5 \times 10^{-4}$, $[H_2SO_4]_B = 1 \times 10^{-2}$, temperature 5.6 °C. (Reproduced with permission from Ouyang and Swinney.[16] © 1991 American Institute of Physics)

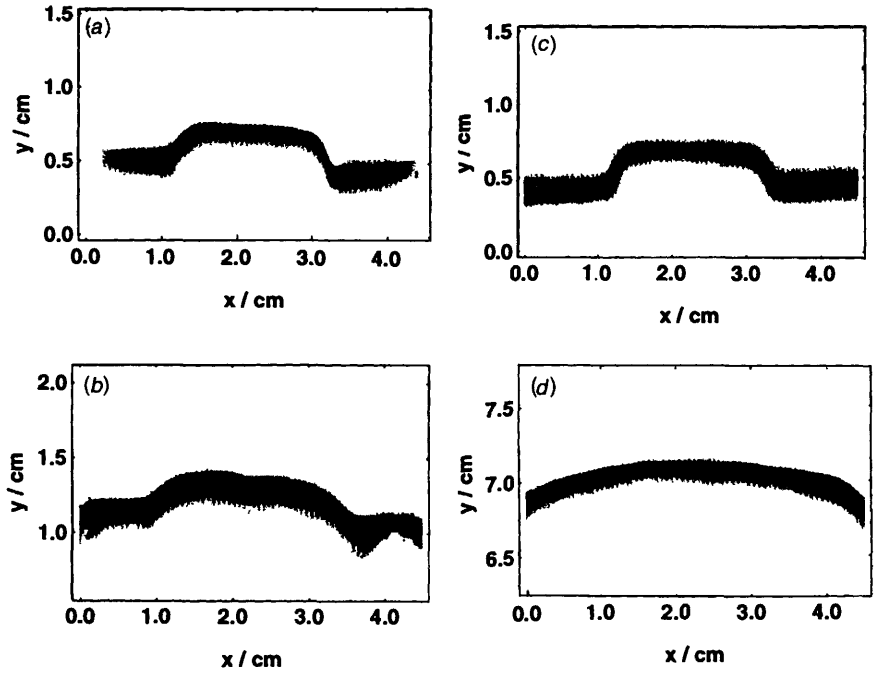

Figure 7 Initial front evolution from a symmetrical perturbation with $[\alpha\text{-cyclodextrin}]_0 = 0.33$ mol l^{-1} for (a) and (b), and $[\alpha\text{-cyclodextrin}]_0 = 0.04$ mol l^{-1} for (c) and (d). (a) Behaviour at $t = 23$ min following initiation at the interface between product and reactant zones; (b) development of front at $t = 343$ min after initiation showing the appearance of a cusp separating two symmetrical cells; (c) behaviour at $t = 23$ min following initiation at the interface between product and reactant zones; (d) development of front at $t = 10$ h after initiation showing the diffusive smoothing of the perturbation. Experimental conditions (concentrations in mol l^{-1}): $[IO_3^-] = 4.8 \times 10^{-3}$, $[As^{III}] = 1.6 \times 10^{-2}$, $[SO_4^{2-}] = 0.32$, $[HSO_4^-] = 4.8 \times 10^{-2}$, $[Ag^+] = 6.5 \times 10^{-5}$, pH = 2.35. (Reproduced with permission from Horvath and Showalter.[20] © 1995 American Institute of Physics)

able reductant (typically HSO_3^- or H_3AsO_3) is known as the Landolt reaction and follows an approximately cubic autocatalytic rate law (2) with $A = IO_3^-$ and $B = I^-$. When performed in a polyacrylamide gel in which α-cyclodextrin, which forms a relatively immobile complex with I^-, has been incorporated, non-planar fronts develop from small perturbations if the concentration of the complexing agent is sufficiently large, but such perturbations decay and a planar front is re-established with lower concentrations, Fig. 7.

If the iodate–reductant system is augmented with ferrocyanide, the kinetics are able to support oscillations in flow reactors. This system has been studied in the Gel Disk Reactor in which complex 'serpentine patterns' have been observed. The 'pattern' is obtained by providing relatively large amplitude perturbations locally at points on the membrane, from which propagating redox fronts emerge. These propagate towards each other until they are separated by a critical distance, when they then stop. The fronts emerging from the various initiation sites eventually produce a structure that fills the spatial domain, with a typical development shown in Fig. 8. Several additional features have also been found, including the 'birth' of new spots as a large spot divides and 'death' as two spots coalesce. Once established by a suitable initial perturbation, this dynamic spatial structure is self-sustaining as long as the flow of reactants is maintained.[21,22]

5 Gel-based Studies of the Belousov–Zhabotinsky reaction

Some of the earliest applications of continuous-flow unstirred reactors based on gels were to studies of the spatial structures of the BZ reaction:[23] the targets and spirals mentioned earlier. The Annual Gel Reactor is formed from a circular annulus of gel with one stream of reactants flowing around the outer circumference and the second stream flowing through the central hole in the gel. A pacemaker site at some point on the gel will initiate a pair of waves, one travelling clockwise, the other counterclockwise. These waves will meet each other at some point across the annular diameter where they will mutually anihilate. (It is a characteristic feature of these chemical waves that they do not pass through each other.) If the transit time for the waves is long compared with the rate of firing of the pacemaker, several pairs of waves may be established at any one time propagating around the gel. By providing a barrier to the propagation of waves close to, and on one side of, the pacemaker, the waves propagating in one of the two senses can be eliminated, leaving say just the clockwise propagating fronts. If the pacemaker can also be then eliminated, these waves will simply continue to run laps around the gel, forming a *chemical pinwheel* as indicated in Fig. 9 (A similar response with a slightly different origin was predicted in Turing's original paper.[4])

Subsequent studies have also exploited the Gel Disk Reactor

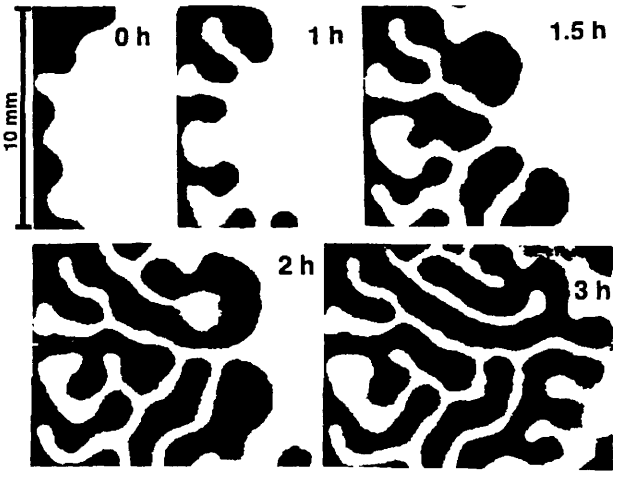

Figure 8 Time evolution of a pattern in the iodate–ferrocyanide–sulfite system initiated by a perturbation with intense ultraviolet light at the left boundary. The pattern achieved 3 h after the localised perturbation was removed is essentially stationary. The pattern was visualised with Bromothymol Blue pH indicator (1.5×10^{-4} mol l^{-1}) so white regions correspond to low pH and black regions to high pH. Experimental conditions (concentrations in mol l^{-1}): $[NaIO_3] = 7.5 \times 10^{-2}$, $[Na_2SO_3] = 8.9 \times 10^{-2}$, $[K_4Fe(CN)_6 \cdot 3H_2O] = 2.5 \times 10^{-2}$, $[H_2SO_4] = 4.5 \times 10^{-3}$, $[NaOH] = 2.5 \times 10^{-4}$; temperature 30.0 ± 1.0 °C. (Reproduced with permission from Lee *et al.*[23] © 1991 The American Physical Society)

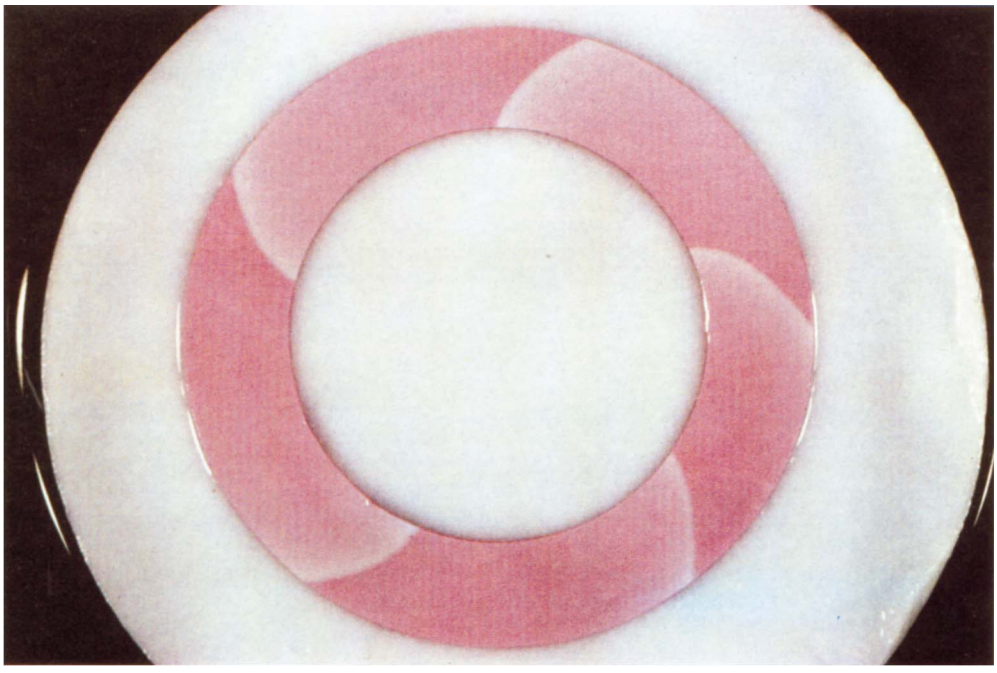

Figure 9 A five-armed pinwheel on a ring-shaped polysulfone membrane 1 h after its initiation. The fixed catalyst is bathoferroin with the ring dimensions inner diameter 24 mm; and outer diameter 37 mm. BZ solution: $[CHBr(COOH)_2] = 0.19$ mol l^{-1}, $[NaBrO_3^-] = 0.12$ mol l^{-1}, $[H_2SO_4] = 0.47$ mol l^{-1} (Reproduced with permission from Noszticzius *et al.*[25] © 1987 Macmillan Magazines Ltd)

using a PVC–silica membrane impregnated with a polyacrylamide gel.[24,25] In the simplest cases, the spiral waves observed are almost identical to those found for similar reactant concentrations in Petri dishes, only now sustained indefinitely by the flows. It is possible to initiate and stabilise a single spiral rather than counter-rotating pairs of spirals. Waves can be initiated in such systems by exposure to UV light and masks can produce waves of varying initial shape. The advantages and challenges presented by the use of gels with reactions such as the BZ system have been considered by Yamaguchi *et al.*[26] Several new approaches, particularly in relation to producing pinwheels, have been developed by Noszticzius.[27]

5.1 Immobilised Catalyst Systems

In the various Gel Reactors described above, all of the components of the BZ system are able to diffuse relatively freely, with diffusion coefficients approaching those appropriate to aqueous solution. With other possible reaction matrices, it is possible effectively to immobilise the redox catalyst, *e.g.* by employing a cation exchange resin either in the form of beads or a membrane. (The redox catalyst is not an autocatalytic or inhibitor species in the BZ reaction so this is a different situation from the Turing systems described in Section 3.) This approach has been particularly exploited by Ken Showalter and Jerzy Masleko in West Virginia.[28] In their original study, a thin layer (0.5 mm) of small cation exchange beads (38 μm to 75 μm diameter) loaded with ferroin was spread in a Petri dish and covered with a 1.6 cm deep solution of the remaining BZ reagents. At low bromate and H^+ concentrations, simple target patterns were established and each bead was uniformly either red or blue depending on its position relative to the waves. As the reactant concentrations were increased, however, more complex responses developed, with waves breaking as they propagated away from their initiation sites, giving rise to asymmetric spiral pairs. These propagated so that the merging wavefront collided with itself, Fig. 10, and eventually produced essentially concentric circular fronts. This is an important aspect: in homogeneous solutions, spiral waves do not evolve spontaneously, but there is a growing body of evidence that shows that they can be expected to develop where inhomogeneities exist. Part of the explanation of this for the bead system relates to the fact that the speed of a wave depends on the curvature of the wave. As the curvature increases (which, for a circular wave, means as the radius decreases), so the speed decreases from that of a plane wave. At some sufficiently small radius, the speed becomes zero and the wave ceases to propagate. This, in turn, means that there is a *critical nucleation size* for BZ waves. The beads at the lower end of the size distribution used in the study of Maselko *et al.* have radii less than this critical size and hence do not initiate waves: only the larger beads act as sources. The critical nucleation size decreases as $[H^+]$ or $[BrO_3^-]$ increase, so at higher concentrations of these reac-

Figure 10 Intensity difference images of a target pattern with a broken spiral centre 132 min after mixing the reagents, produced from two images collected at 440 nm and 10.0 s apart. The dark bands represent the distance that the wave has travelled between image shots. Image size 19.3 × 19.3 mm. Experimental conditions: $[KBrO_3] = 0.3$ mol l^{-1}, $[H_2SO_4] = 0.25$ mol l^{-1}, $[CH_2(COOH)_2] = 2.5 \times 10^{-2}$ mol l^{-1}, 1.0×10^{-5} mol g^{-1} immobilised on > 400 mesh size Bio-Rad Analytical Grade 50W-X4 cation exchange resin. (Reproduced with permission from Maselko *et al.*[28] © 1989 The American Chemical Society)

tants the system becomes more 'active' with more beads able to act as initiation sites. Small beads and vacancies in the layer due to imperfect packing, however, can act as 'wave breaks.' The random arrangement of the beads in the layer means that wave breaks are likely to occur in some directions but not others, giving rise to the formation of wave 'ends' that develop into spirals.

With larger cation exchange beads, 0.5—1.4 mm diameter, spirals can actually be observed unwinding and then rewinding as they propagate over the surface of individual beads in the form of a *chemical rotor*. The precise form of these waves has provided a challenge to theory from which a different geometric form has been predicted.

5.2 Immobilization on Membranes

Cation exchanges can also be obtained in thin films. An example is Nafion, a perfluorinated sulfonic acid derivative used widely in the electrolytic production of NaOH. If a Nafion membrane is loaded with ferroin and immersed in the BZ reagents, spiral waves can develop spontaneously on the solution–membrane interface. The solution can be fed through the reactor so providing a continuous feed of the reagents and the reaction is thus sustained over an extended period. The spirals propagate more slowly than in solution, partly reflecting the lower diffusifity of $HBrO_2$ in the membrane. The anionic reactants, BrO_3^- and Br^-, are unable to penetrate the Nafion matrix, which has a net negative charge, so the reaction is restricted to the membrane surface. Spiral waves can develop on each of the surfaces of the thin strips[29] and, most interestingly, the diffusion of neutral species such as the autocatalyst $HBrO_2$ through the matrix, from one face to the other, allows the spatial structures to communicate. The strength of this coupling can be varied by changing the ferroin loading (high loading gives weak coupling). Coupling between two layers of waves can also arise in gel-based BZ systems in which there is an O_2 concentration gradient,[30] as oxygen reacts with some of the organic intermediates. Some very complex entrainment patterns have been observed in this configuration, Fig. 11, and this form of coupling is of real interest as a simple analogue of the chemical signalling that occurs across biological membranes *in vivo*.

In a simpler arrangement,[31] in which only one membrane surface is in contact with the solution, the initial development of spiral waves in the region behind an initial reaction front has been followed. The development of the broken waves which subsequently evolve into rotating spirals can be explained in terms of the spatially inhomogeneous *recovery* of the membrane. Recovery corresponds to the system returning to the reduced state some time after the oxidation wave has passed over a given point in the membrane and so locations further behind the advancing front are more recovered than those over which the front has passed more recently. Only once the system is sufficiently recovered can it support the passage of another wave, so if a stimulus is applied relatively close to the back of a wave, it is only likely to initiate waves propagating away from the original front and so produce a pair of wave ends that will evolve into spirals. This phenomenon is known as *vulnerability* in the cardiac literature where it is strongly implicated in the development of spiral and other types of wave structure associated with cardiac arrhythmias.

6 Further Exploitation of the Techniques

The various experimental methods and techniques developed for spatial systems over the past ten years provide many more general possibilities for studying reactions in the reaction–diffusion (or other mode of transport) contexts. The classic Liesegang Ring phenomenon involves a different mechanism from the Turing instability: a periodic precipitation of an insoluble salt formed as one chemical species diffuses through a gel impregnated with a second reactant has recently been revisited.[32] Some complex patterns

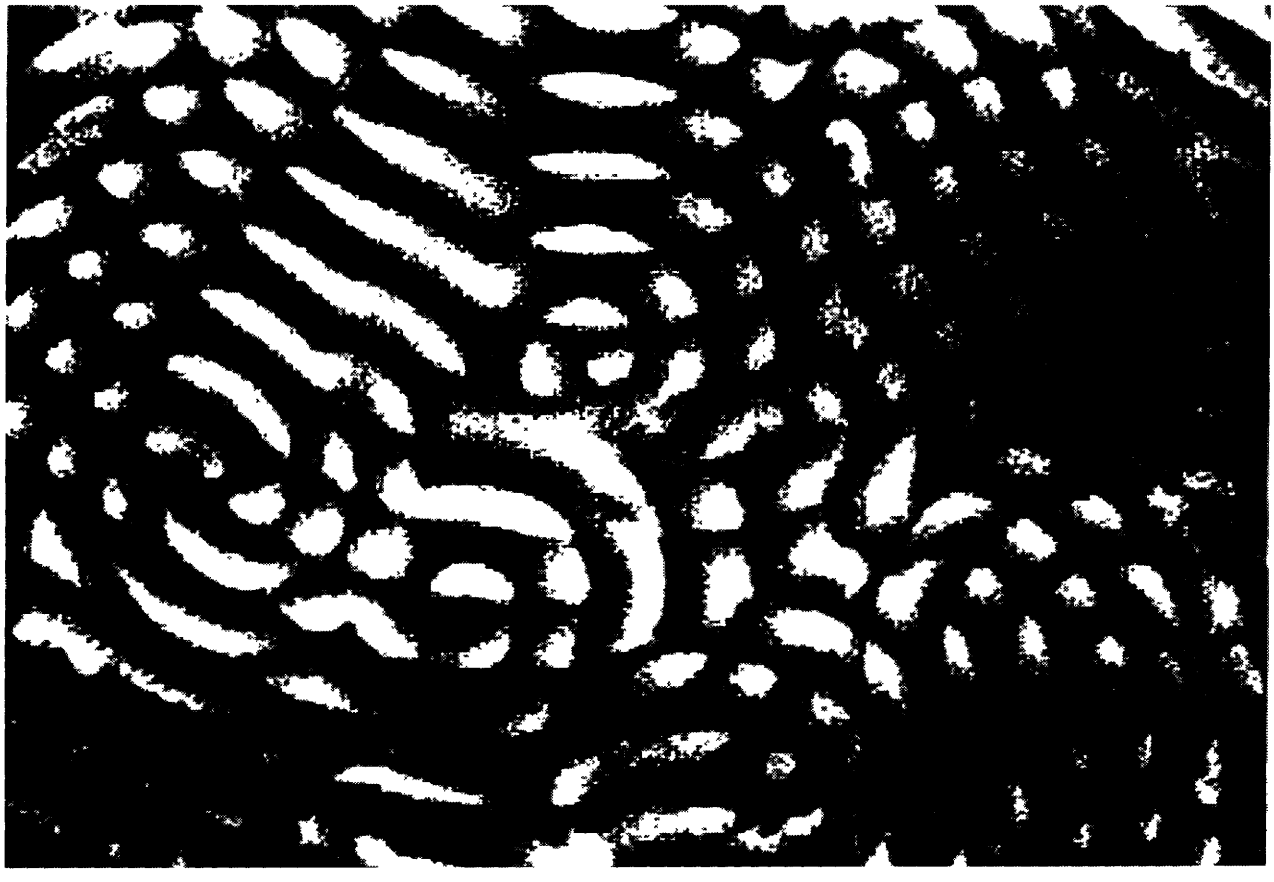

Figure 11 Chemical waves propagating on the surface of a ferroin-loaded Nafion membrane suspended in a cstr pumped with BZ reaction mixture. Image shows the intensity of light transmitted through a membrane 0.18 mm in thickness, 4.5 h after initiation, residence time of 56.93 min; field of view is 6.3 × 4.7 mm. Nafion loading 38.7%. Reactant concentrations (mol l^{-1}) in cstr: $[NaBrO_3] = 0.19$, $[H_2SO_4] = 0.24$, $[CH_2(COOH)_2] = 1.9 \times 10^{-2}$, [ferroin] $= 5.8 \times 10^{-5}$, $[KBr] = 8.7 \times 10^{-4}$ temperature 25.0 °C (Reproduced with permission from Winston *et al.*[29] © 1991 Macmillan Magazines Ltd)

include radial dislocations in the concentric precipitation rings obtained in a thin layer of gel into which a high concentration of one of the chemicals is introduced at a 'point' Other patterns include helical precipitation bands in which the precipitate pitches on a screw axis as it propagates down a test tube On the basis of detailed experimental observations, a more comprehensive theory has been developed which combines the original Ostwald hypothesis based on supersaturation and nucleation with the mechanism proposed by Ortoleva involving a reasonably homogeneous initial precipitation with subsequent spatial development due to the growth of larger particles at the expense of smaller ones (the Lifshitz–Slyozov instability)

If the ferroin redox catalyst in the BZ reaction is replaced by the $Ru(bipy)_3^{2+}$ (bipy = 2 2′-bipyridine) complex, the ability of the matrix to support wave propagation can be varied by illumination[33] which produces an electronically excited form of the catalyst that reacts directly with bromate ion to form the inhibitor bromide ion locally This allows for an element of 'spatial control' over the reaction and has been exploited to remove spiral centres by causing them to collide with each other or with the reactor walls and to produce novel spatial patterns with multi-armed spirals

Intricate spatial domains can be readily constructed with the redox catalyst either preloaded onto a membrane that is then cut into the desired 'floor plan' or, most imaginatively, by replacing the ink in a pen plotter with ferroin and then drawing complex patterns onto membrane supports that are then immersed in the BZ reagent In this way, the propagation of waves through mazes can be used to find the shortest path subject to various constraints or the fundamental building blocks, logic gates, for construction of a chemical computer[34,35]

The understanding developed through such studies should help other situations, such as the transport and reaction of species incorporated into water droplets or small ice particles of relevance in the cloud chemistry associated with acid rain formation We can also expect to see attacks on more complex transport problems such as those in combustion where the chemistry interacts with and causes significant convective effects even in the absence of imposed flows Perhaps the main area of application, and that in which Turing's speculations were first proposed, for these advances in knowledge, however, will lie in their significance for biological systems in which chemical kineticists, especially those with backgrounds that encompass nonlinear feedback, have much to contribute

7 References

1 *Chemical Waves and Patterns*, ed R Kapral and K Showalter Kluwer, Dordrecht, 1995
2 *Dynamism and Regulation in Nonlinear Chemical Systems* (*Physica* **D84**), ed M A Marek, S C Muller, T Yamaguchi and K Yoshikawa North Holland, Amsterdam, 1995
3 S K Scott, *Oscillations Waves and Chaos*, Oxford University Press, 1994
4 A M Turing, *Philos Trans Roy Soc* , 1952, **B327**, 37
5 A T Winfree, *Science*, 1974, **175**, 634
6 S Nettesheim, A von Oertzen, H H Rotermund and G Ertl, *J Chem Phys* , 1993, **98**, 9977
7 H Pearlman, *Combustion and Flame*, 1996, in press
8 J D Murray, *Mathematical Biology*, Springer, Berlin, 1990
9 L Glass and M C Makey, *From Clocks to Chaos the Rhythms of Life*, Princeton University Press, 1988
10 P De Kepper, J Boissonade and I R Epstein, *J Phys Chem* , 1990, **94**, 6525
11 I Lengyl, G Rabai and I R Epstein, *J Am Chem Soc* , 1990, **112**, 4606, 9104
12 S C Muller, Th Plesser and B Hess, *Science*, 1985, **230**, 661, *Naturwissenschaften*, 1986, **73**, 165
13 V Castets, E Dulos, J Boissonade and P De Kepper, *Phys Rev Lett* , 1990, **64**, 2953
14 I Lengyl and I R Epstein, *Science*, 1991, **251**, 650
15 P De Kepper, V Castets, E Dulos and J Boissonade, *Physica*, 1991, **D49**, 161
16 Q Ouyang and H L Swinney, *Chaos*, 1991, **1**, 411
17 Q Ouyang and H L Swinney, *Nature*, 1991, **352**, 610
18 Z Noszticzius, Q Ouyang, W D McCormick and H L Swinney, *J Phys Chem* , 1992, **96**, 6302
19 K Agladze, E Dulos and P De Kepper, *J Phys Chem* , 1992, **96**, 2400
20 D Horvath and K Showalter, *J Chem Phys* , 1995, **102**, 2471
21 K J Lee, W D McCormick, J E Pearson and H L Swinney, *Nature*, 1994, **369**, 215
22 K J Lee, W D McCormick, Q Ouyang and H L Swinney, *Science*, 1993, **261**, 192
23 Z Noszticius, W Horsthemke, W D McCormick, H L Swinney and W Y Tam, *Nature*, 1987, **329**, 619
24 W Y Tam, W Horsthemke, Z Noszticzius and H L Swinney, *J Chem Phys* , 1988, **88**, 3395
25 G Kshirsagar, Z Noszticzius, W D McCormick and H L Swinney, *Physica*, 1991, **D49**, 5
26 T Yamaguchi, L Kuhnert, Zs Nagy Ungvarai, S C Muller and B Hess, *J Phys Chem* , 1991, **95**, 5831
27 A Lazar, Z Noszticzius, H D Forsterling and Zs Nagy Ungvarai, *Physica*, 1995, **D84**, 112
28 J Maselko, J S Reckley and K Showalter, *J Phys Chem* , 1989, **93**, 2774
29 D Winston, M Arora, J Maselko, V Gaspar and K Showalter, *Nature*, 1991, **351**, 132
30 A M Zhabotinsky, S C Muller and B Hess, *Physica*, 1991, **D49**, 47
31 S K Scott, J D B Smith and B W Thompson, *J Chem Soc , Faraday Trans* , 1996, **92**, 325
32 A A Polezhaev and S C Muller, *Chaos*, 1994, **4**, 631
33 M K R Reddy, Zs Nagy Ungvarai and S C Muller, *J Phys Chem* , 1994, **98**, 12255
34 O Steinbock and K Showalter, *Science*, 1995, **269**, 418
35 A Toth and K Showalter, *J Chem Phys* , 1995, **103**, 2058